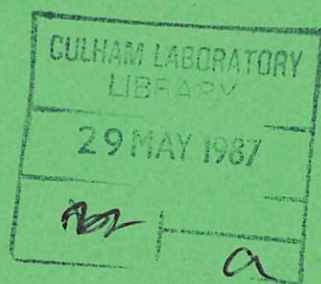




UKAEA

Preprint

CULHAM LIBRARY
REFERENCE ONLY



NUMERICAL SIMULATION OF TWO-DIMENSIONAL TRANSIENT MULTI-PHASE MIXING

D.F. Fletcher

A. Thyagaraja

CULHAM LABORATORY

Abingdon Oxfordshire
1987

This document is intended for publication in a journal or at a conference and is made available on the understanding that extracts or references will not be published prior to publication of the original, without the consent of the authors.

Enquiries about copyright and reproduction should be addressed to the Librarian, UKAEA, Culham Laboratory, Abingdon, Oxon. OX14 3DB, England.

NUMERICAL SIMULATION OF TWO-DIMENSIONAL TRANSIENT MULTI-PHASE MIXING

D.F. Fletcher and A. Thyagaraja

Culham Laboratory, Abingdon, Oxon. OX14 3DB, England

(Paper to be presented at The 5th International Conference on Numerical
Methods for Thermal Problems, Montreal, Quebec, June 29 - July 3, 1987)

February 1987

NUMERICAL SIMULATION OF TWO-DIMENSIONAL TRANSIENT MULTIPHASE MIXING

D. F. Fletcher and A. Thyagaraja

Culham Laboratory, Abingdon, Oxfordshire, OX14 3DB, U.K.

SUMMARY

In this paper we describe a finite-difference model of multiphase mixing. The model is applicable to the study of a hot fluid poured into a cold vaporisable fluid. We represent this situation using the continuum equations of multiphase flow and give a description of the equations to be solved and the boundary conditions used. The outline of the numerical solution scheme is described and the new features we have developed are highlighted. Emphasis is placed on the need to ensure qualitative consistency of the finite difference scheme with the properties of the differential equations. Finally, we present some sample calculations showing that the model gives good general agreement with experimental data.

1. INTRODUCTION

The calculation of multiphase flow is of considerable interest in the nuclear and process industries. A particular application, the modelling of transient buoyancy-driven multiphase mixing which occurs on relatively slow timescales (~ 1 second), is the subject of this paper. For example, we are concerned with the modelling of the behaviour of a jet of hot melt poured into a pool of cold vaporisable liquid (usually water). This situation may occur in certain accidents within the metal casting industry or may arise in the progression of hypothetical accidents in the nuclear industry if core material melts and pours into water [1].

This problem is particularly difficult to model since the melt may be at a very high temperature (~ 3500 K) so that the heat transfer rate to the cold liquid (water in our application) could be of the order of 5 MW/m^2 from thermal radiation alone, leading to very high vapour production rates. A recent review [2] of the available models of this process

has identified the need to develop a transient, 3-component (melt (M), water (W), steam (S)) multiphase flow model. To be a useful tool the model needs to have the following properties:

- (a) The resulting computer code must be stable, robust and ensure that quantities such as volume fractions always remain positive.
- (b) It must be able to work with virtually arbitrary constitutive relations for interphase drag, heat-transfer rates and melt particle fragmentation.
- (c) There is no great need for a high order accuracy in the finite difference scheme since many of the constitutive relations are only known approximately and the experimental data are global measurements with substantial uncertainties.
- (d) It must be relatively cheap to use so that the effect of uncertain parameters can be scoped.

In the remainder of this paper we describe the model, finite difference equations and solution procedure developed to satisfy the above aims, together with the simulation of a particular experiment. Due to the short length of this paper we draw heavily on our earlier work described in references 3,4 and 5.

2. FORMULATION OF THE MATHEMATICAL MODEL

We assume that mixing takes place axisymmetrically in a right-circular cylinder of radius R , height H , open at the top. The flow velocities are small enough to allow the incompressible approximation, so that the mass densities ρ_M , ρ_W and ρ_S may be taken as constants. This results in a set of equations of the form

$$\frac{\partial}{\partial t}(\alpha_i \phi_i) + \frac{1}{r} \frac{\partial}{\partial r}(r U_i \alpha_i \phi_i) + \frac{\partial}{\partial z}(V_i \alpha_i \phi_i) = S \phi_i \quad (1)$$

where α_i is the volume fraction, U_i is the horizontal velocity (in the r -direction) and V_i is the vertical velocity (in the z -direction) of species i ($i = M, W, S$). Table 1 below lists the variables ϕ_i and the source terms for the water species equations, plus the melt enthalpy and melt length-scale equations.

<u>Equation</u>	<u>ϕ</u>	<u>source term</u>
Conservation of water mass	1	\dot{m}_W/ρ_W
Conservation of radial momentum	$\rho_W U_W$	$-\alpha_W \frac{\partial \bar{p}}{\partial r} - \alpha_W \frac{\partial \chi}{\partial r}$ $+F_{WM}^r + F_{WS}^r + F_{Wm}^r$
Conservation of axial momentum	$\rho_W V_W$	$-\alpha_W \frac{\partial \bar{p}}{\partial z} + g\alpha_W\alpha_M(\rho_M - \rho_W)$ $+g\alpha_W\alpha_S(\rho_S - \rho_W)$ $+F_{WM}^z + F_{WS}^z + F_{Wm}^z$
Melt enthalpy	$\rho_M H_M$	$-\dot{m}_S h_{fg}$
Melt length-scale	L_M	$-\alpha_M(L_M - L_{crit})/\tau_L$

Table 1 : Coefficients and source terms in the conservation equations.

In addition to the above equations the volume fractions must satisfy the constraint

$$\alpha_M + \alpha_W + \alpha_S = 1 \quad (2)$$

which implies the following elliptic constraint,

$$\frac{1}{r} \frac{\partial}{\partial r} (r(\alpha_M U_M + \alpha_W U_W + \alpha_S U_S))$$

$$+ \frac{\partial}{\partial z} (\alpha_M V_M + \alpha_W V_W + \alpha_S V_S) = \frac{\dot{m}_S}{\rho_S} - \frac{\dot{m}_W}{\rho_W} \quad (3)$$

The above equation allows the common pressure to be determined, as will be illustrated in section 3.

2.1 Form of the source term

In this section we describe the source terms, together with the necessary constitutive relations needed to close the problem. We assume that $\dot{m}_M = 0$ so that there are no internal sources or sinks of melt in the solution domain. Melt is either present initially in the solution domain or is injected at a boundary. We assume that there is no condensation of steam (i.e. $\dot{m}_S > 0$), since in all problems of interest to us the water is saturated. In addition, we have $\dot{m}_W + \dot{m}_S = 0$ and set

$$\dot{m}_W = -\alpha_W \alpha_M 6h(T_M - T_W)/L_M h_{fg} \quad (4)$$

where we have assumed the melt to be in the form of spheres of diameter L_M . T_M and T_W are the melt and water temperatures, h_{fg} is the latent heat of vaporisation and h is the appropriate heat transfer coefficient (usually radiation plus film boiling).

In the momentum equations we work with a reduced pressure, defined by

$$\bar{p} = p - \chi = p - \int_z^H g(\alpha_M \rho_M + \alpha_W \rho_W + \alpha_S \rho_S) dz \quad (5)$$

Thus the usual axial momentum source term $-\alpha_W \frac{\partial p}{\partial z} - \alpha_W \rho_W g$ takes the form given in table 1 and $\frac{\partial \chi}{\partial r}$ terms appear in the radial momentum equations. The terms F_{WM}^r and F_{WM}^z represent interphase drag between the melt and water in the r and z directions respectively. These terms were modelled using the drag law proposed by Harlow and Amsden [6] and their exact form is given in [5]. The important point to note is that

$$F_{WM}^r \equiv D_{WM}^r(\alpha_M, \alpha_W, L_M, L_W, U_M, U_W, V_M, V_W)(U_M - U_W) \quad (6)$$

so that provided $D_{WM}^r = D_{MW}^r$ Newton's third law is satisfied. The terms F_{WM}^z etc. represent evaporation reaction forces and are not present in the melt equation. These take the form

$$F_{WM}^z = -\dot{m}_S U_W, \quad F_{SM}^z = \dot{m}_S U_W \quad (7)$$

In the enthalpy equation the kinetic energy of the melt and terms arising from pressure and drag work have been neglected, since they are small compared to the thermal energy terms. The source term ensures that the melt cools by an amount consistent with the heat used to produce vapour. The melt temperature is determined from the enthalpy by using a suitable caloric equation of state. In the melt length-scale equation the source term causes the melt length-scale to reduce to L_{crit} with a fragmentation rate $1/\tau_L$.

2.2 Boundary and initial conditions

We assume that $U_i = 0$ on $r = 0$, $U_i = 0$ on $r = R$, $V_i = 0$ on $z = 0$. At the top ($z = H$) we set $U_i = 0$ and

$\frac{\partial v_W}{\partial z} = \frac{\partial v_M}{\partial z} = 0$. A uniform steam velocity outlet profile is set with the flow rate determined from the volume integral of equation (3). At $t = 0$ an initial velocity and volume fraction field is specified together with the length-scale and temperature of each species. Any melt injected into the

solution domain is given a specified velocity, length-scale and enthalpy.

3. SOLUTION SCHEME

Only the outline of the solution scheme is presented here, full details are given in references 3,4 and 5. The equations given in the previous section were finite differenced on a staggered grid. All convective terms were upstream differenced for stability. The solution procedure is as follows:

- (a) Time advance the α_M equation to get $\alpha_M(t+\Delta t)$ using the melt velocity and α_M fields at time t .
- (b) Similarly time advance L_M and H_M and determine T_M using the caloric equation.
- (c) Time advance the α_W equation treating the source term implicitly.
- (d) Determine $\alpha_S = 1 - \alpha_W - \alpha_M$
- (e) Determine new velocity fields using the pressure field at time t .
- (f) Substitute the new velocity and volume fraction fields into the finite differenced form of equation (3) to determine the local continuity error.
- (g) If this error is too large update the pressures using Newton's method, go back to step (e) and repeat the procedure using the modified pressure field. Iterate steps (e) \rightarrow (g) until the local continuity errors (suitably normalised) are below the desired accuracy level.

Typically after 2 iterations the above procedure converges and the code steps forward in time again. The chosen method of time advancing the α 's ensures that they remain positive and if the continuity error is reduced to a suitably small value they remain less than unity [3]. For stability we require the Courant number $(\text{Max} (\frac{V_i \Delta t}{\Delta z}, \frac{U_i \Delta t}{\Delta r}))$ to be less than unity and for accuracy we require the product of any rate parameter and the time-step to be less than unity e.g. $\Delta t / \tau_L \ll 1$.

In the momentum equations the velocities of all species are coupled at each grid location due to the drag terms. Thus at each grid point we invert a 3×3 matrix to obtain the new velocities of all 3 species simultaneously. This procedure ensures that even with extremely large drag forces Newton's

third law is exactly satisfied. A semi-implicit scheme is used for accuracy.

The pressure correction is carried out by first correcting the pressure level in vertical slabs. The pressure is then corrected locally within each slab. Thus we avoid the need to solve Poisson's equation directly but instead use a TDMA solution for the blocks and then a TDMA solution within each block.

4. RESULTS

The code has been extensively tested on model problems and has been found to give grid independent solutions and to predict solutions which depend continuously on the initial data. It has been used to simulate the one-dimensional mixing of heated ball-bearings with water [4] and has been used to model a two-dimensional mixing experiment carried out at Argonne [5]. In this section we present a further comparison with the Argonne experiment (CWTI-9) in which the melt length-scale is evolved with time, unlike in our earlier work where we assumed pre-fragmented melt of a fixed size. The experimental geometry is shown in Figure 1 below.

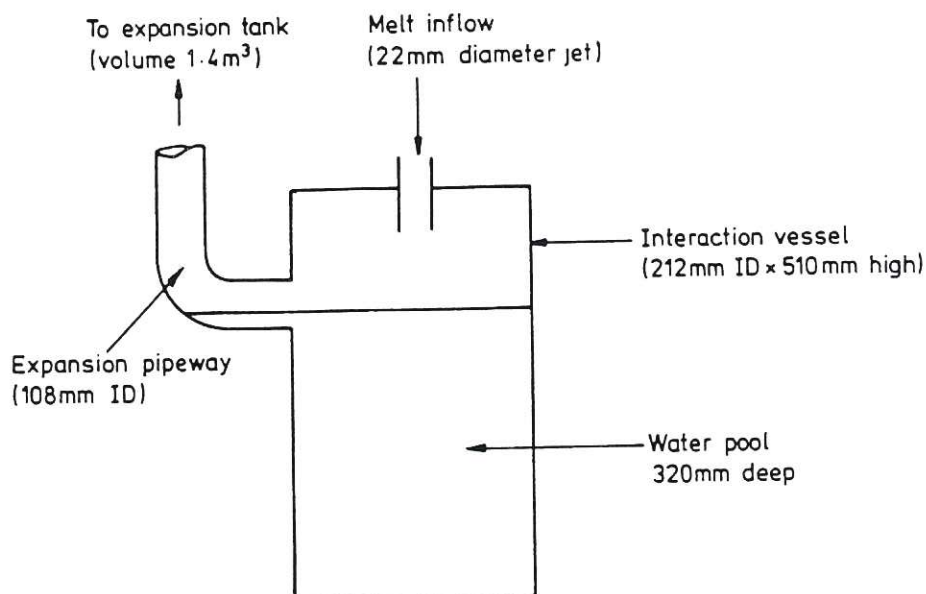


Fig 1. Illustration of the experimental geometry.

A full description of the experiment and chosen constitutive relations is beyond the scope of this paper. The experiment is reported in reference 7 and we use the same constitutive relations as those used in our previous calculations (see section 6.1 of reference 5). A 10×10 grid and a time-step of 5×10^{-6} s was used. Briefly, the experiment consisted of the injection of molten corium into a vessel partially filled with water. The vessel was closed except for a pipeway on the side which allowed the steam produced to be collected in a tank (see figure 1). In our calculations the vessel is assumed to be open at the top (we cannot model 3-D effects) and we determine how much steam is produced. In this way we can use our data to generate a pressure transient similar to that measured in the expansion vessel by the experimenters.

A comparison of the calculated pressurization results for three different assumptions about the melt fragmentation parameters, (case 1 $\equiv L_{crit} = 1\text{mm}$, $\tau_L = 0.02\text{s}$, case 2 $\equiv L_{crit} = 2\text{mm}$, $\tau_L = 0.0033\text{s}$, case 3 $\equiv L_{crit} = 2\text{mm}$, $\tau_L = 0.02\text{s}$), is shown in figure 2. The initial melt length-scale was set equal to the pour diameter. The plot shows that the experimental data is well-fitted for this range of parameters.

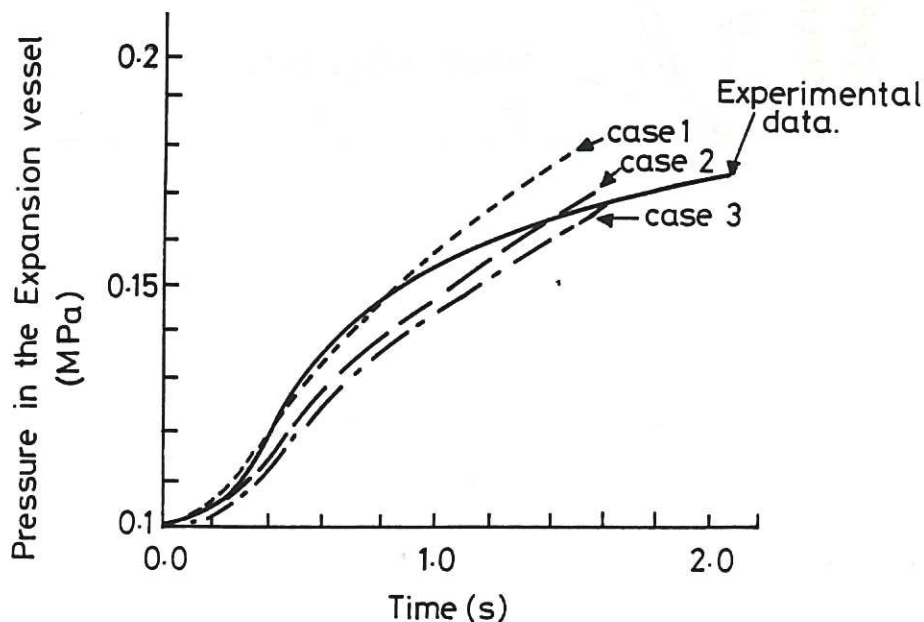


Fig.2 A comparison of the predicted and measured vessel pressurisation data.

These are consistent with the experimentally determined particle size distribution and break-up rates resulting from hydrodynamic instabilities. The agreement is less good at later times as the present simulation does not allow for vapour condensation. However, comparison of the present results with the simulation presented in reference 5 shows that allowing for a finite melt fragmentation rate improves the agreement with the experimental data.

Figure 3 shows the steaming rate and the experimentally measured corium inflow rate as a function of time. This

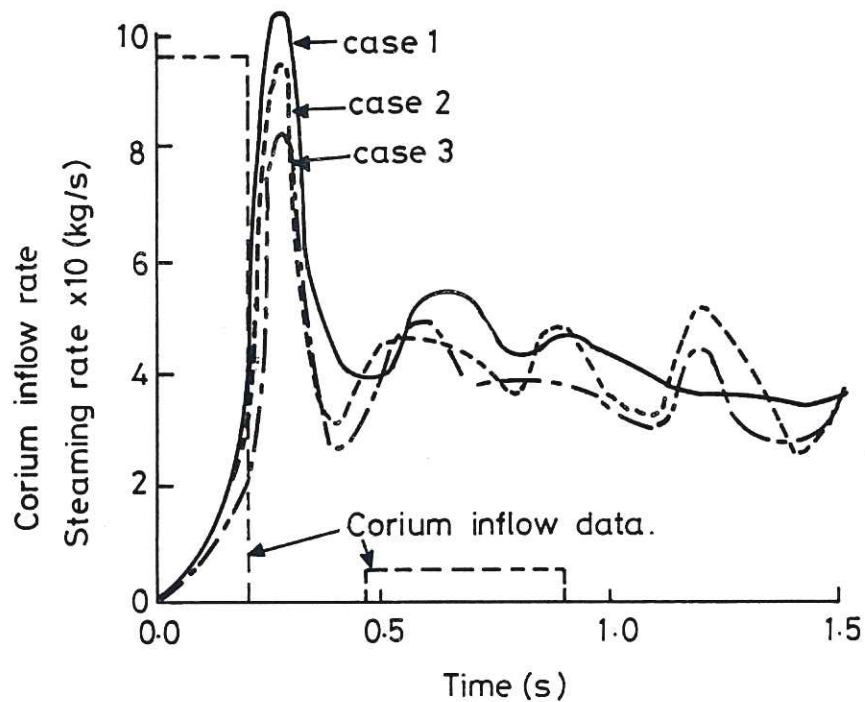


Fig.3. The transient steaming rate.

figure shows how the fragmentation parameters affect steam production, with the peak vapour production occurring when most of the melt has entered the water pool, at about 0.25s after melt release. At later times the steam production rate oscillates because steam sweeps melt out of the water, the steam production rate falls and then the melt falls back into the water leading to further vapour production.

Figure 4 shows volume fraction and velocity field plots for the melt and water 0.1s after melt release. The plots are for case 1 but all cases show the same qualitative features. The plots show the melt entering the water pool as a jet and then spreading as it mixes with water. The water level rises due to the entry of melt and steam production. The water velocity plot shows the level swell rate to be about 0.5 m/s and also shows that some water is carried along with the

leading edge of the jet. At later times vapour production becomes very rapid and the water pool 'froths up' to fill the

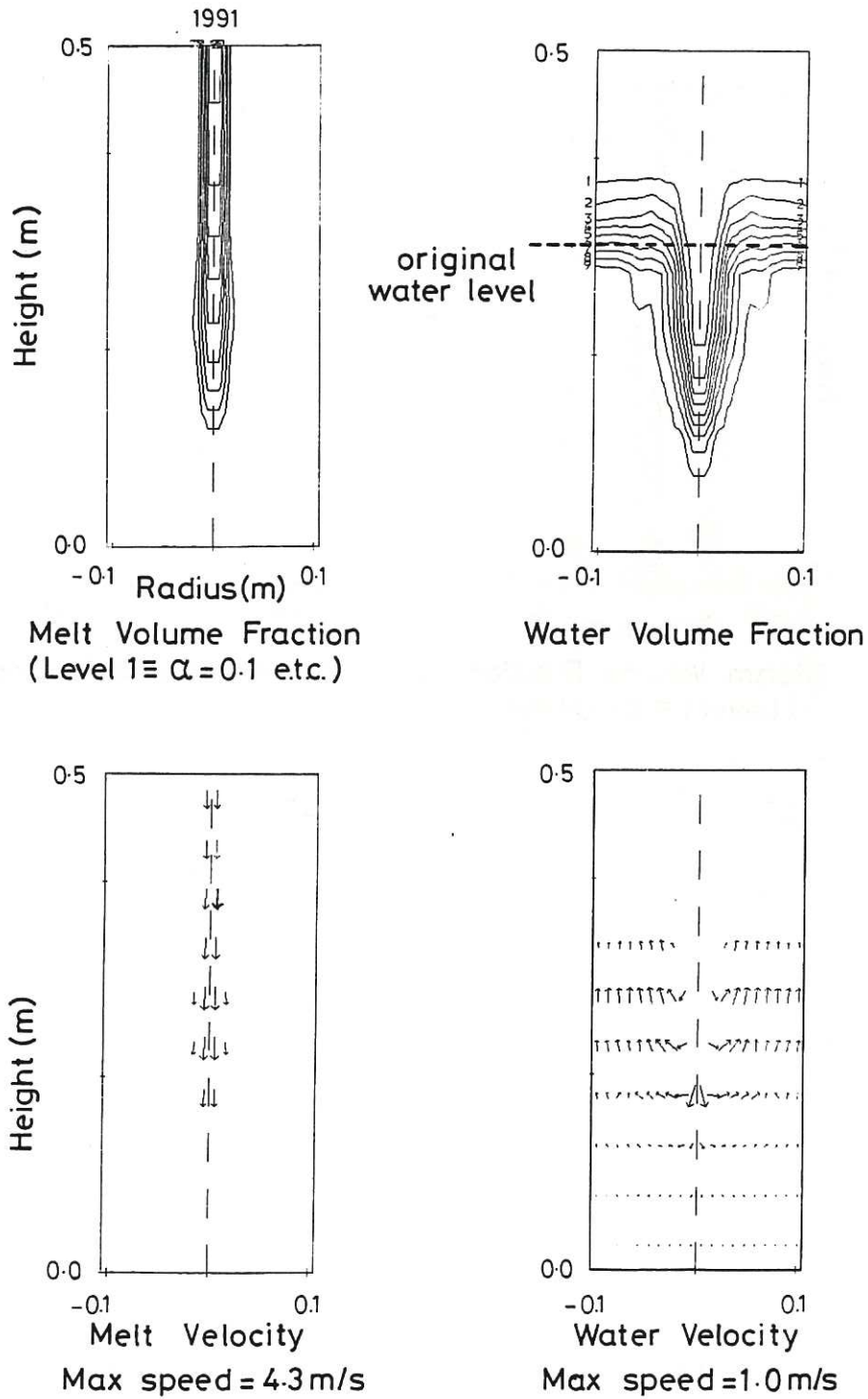


Fig.4. Volume fraction & velocity fields at $t=0.1s$.

vessel. Figure 5 shows volume fraction and velocity plots for water and steam at a time of 0.2s. The figure shows that most of the water has been pushed to the side of the vessel and steam is exiting the system with a peak velocity of 93 m/s.

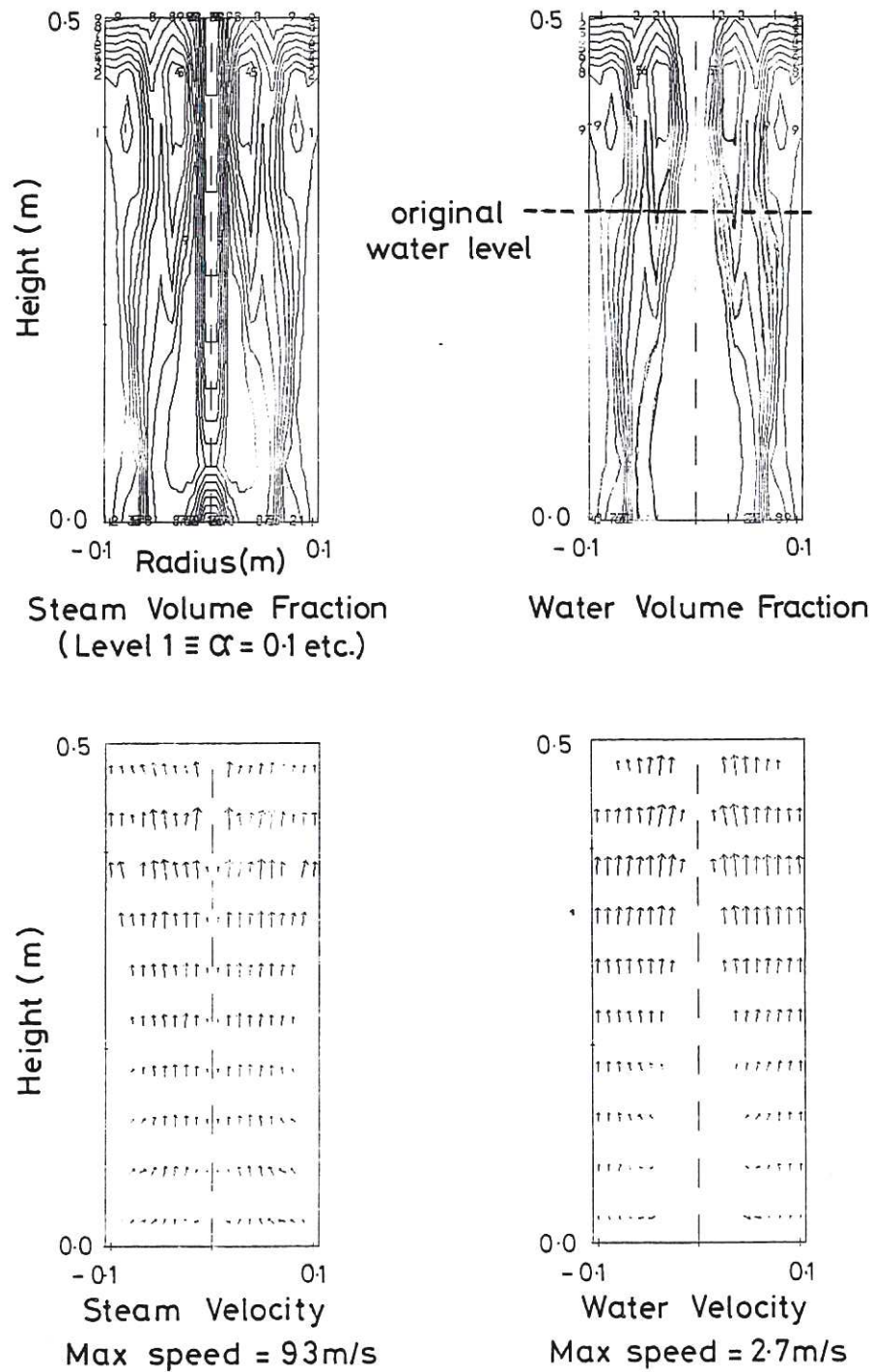


Fig.5. Volume fraction & velocity fields at $t=0.2\text{s}$.

In the experiment 13% of the corium and 36% of the water were estimated (by the experimenters) to have been expelled from the mixing vessel. Table 2 below shows the calculated values for the three different simulations performed.

<u>Case</u>	% melt expelled	% water expelled
1	26	93
2	17	73
3	12	79

Table 2: Melt and Water 'Sweep-out' Data

The data in the above table shows that the melt 'sweep-out' is most accurately modelled for a final particle size of 2mm. However, the model predicts that approximately twice as much water was 'swept-out' as observed in the experiments. This difference could be due to differences in the experimental and modelling geometries (in the experiment the steam has to flow around a bend so this may cause both water and melt to be deposited by the flow) or it may be due to the chosen steam-water drag law. However, the simulation shows good qualitative agreement with the experimental data and highlights the importance of the 'sweep-out' phenomena.

5. DISCUSSION

In this paper we have described a multiphase flow model of the mixing of a hot fluid jet with a cold vaporisable liquid. At the beginning of the paper we set out four guiding aims for producing such a model. These have been largely realised. The computer code is stable and robust due to the choice of method used to finite difference the conservation equations and the choice of solution scheme. The constitutive relations need only satisfy very general properties which are required on physical grounds alone, for example, the drag laws must satisfy Newton's third law. The code gives generally good agreement with the limited available experimental data. Finally, although each computation uses typically 3500 cpu seconds on a CRAY-XMP, this is still relatively cheap and far less costly than experimental studies of mixing. Thus the code can be used to determine the important parameters and effects which can then be examined in detailed experimental studies. To the best of our knowledge the code described in this paper is unique in its ability to model experiments of this type.

ACKNOWLEDGEMENT

The authors would like to thank Mrs G. Lane for making such a good job of typing this manuscript.

REFERENCES

1. CRONENBERG, A.W. - Recent Developments in the Understanding of Energetic Molten Fuel-Coolant Interactions. Nuclear Safety, 21, 319-337 (1980)
2. FLETCHER, D.F. - A Review of Coarse Mixing Models. Culham Laboratory report CLM-R251 (1985)
3. THYAGARAJA, A., FLETCHER, D.F. and COOK, I. - One Dimensional Calculations of Two-phase Mixing Flows. Int. J. Numer. Methods Eng., 24, 459-469 (1987)
4. FLETCHER, D.F. and THYAGARAJA, A. - Numerical Simulation of One-dimensional Multiphase Mixing. Culham Laboratory preprint CLM-P776 (1986)
5. THYAGARAJA, A. and FLETCHER, D.F. - Buoyancy-driven, Transient, Two-dimensional Thermo-hydrodynamics of a Melt-water-steam Mixture. Culham Laboratory preprint CLM-P790 (1986)
6. HARLOW, F.H. and AMSDEN, A.A. - Flow of Interpenetrating Material Phases. J. Comp. Phys., 18, 440-465 (1975)
7. SPENCER, B.W., MCUMBER, L., GREGORASH, D., AESCHLIMANN, R. and SIENICKI, J.J. - Corium Quench in Deep Pool Mixing Experiments. Paper presented at the National Heat Transfer Conference, Denver, Colorado, U.S.A. August (1985)

